# Numerical Simulation of Trapped-Electron Instabilities in Toroidal Geometry

C. Z. Cheng and H. Okuda
*Plasma Physics Laboratory, Princeton University, Princeton, New Jersey 08540*
(Received 14 June 1978)

Dissipative trapped-particle instabilities are studied by means of three-dimensional particle simulations in toroidal geometry. In the linear stage, growth rates of the unstable modes and the radial and poloidal ballooning mode structures observed in the simulation agree reasonably well with linear theory. In the nonlinear stage, the ballooning effect diminishes because of the generation of strong plasma turbulence resulting in the broad frequency spectrum and convective cells consistent with experimental observations.

The importance of low-frequency drift-type instabilities has long been recognized in relation with the anomalous plasma transport in toroidal confinement devices.[1] At present, a fairly complete linear theory for such instabilities in toroidal systems has been developed.[2] However, nonlinear behavior of these instabilities and the resultant anomalous particle and energy diffusion have not been well understood. Recently, it has been demonstrated that three-dimensional particle simulations[3] are useful for understanding the strong plasma turbulence and the anomalous diffusion due to collisionless drift instabilities.[4] In particular, it was found that the collisionless drift instabilities can generate strong turbulence and convective cells which in turn enhance particle diffusion.

In this paper, we report on our recent simulation studies of the dissipative trapped-electron instabilities using a three-dimensional toroidal plasma model.[3] It will be shown that, in the earlier stage of the instabilities, the simulation results agree reasonably well with the linear theory. In particular, we observe the ballooning effect on the poloidal mode structure of the unstable modes. In the nonlinear stage, however, the ballooning effects diminish due to the generation of strong plasma turbulence and broad spectrum consistent with the experimental observations.[1]

The simulation model is a torus in an external magnetic field given by $\vec{B}=B_\varphi\hat{e}_\varphi+B_\theta\hat{e}_\theta$, where $B_\varphi=B_\varphi^{(0)}/(1+\epsilon\cos\theta)$ is the toroidal field and $B_\theta=(\epsilon/q)B_\varphi^{(0)}$ is the poloidal field. $\epsilon\equiv r/R_0$ is the inverse aspect ratio, $\varphi$ is the toroidal angle, $\theta$ is the poloidal angle measured from the outside towards the inside of a torus, and $r$ and $R_0$ are the minor radius and major radius of the torus. Full Lorentz force is employed for the ion dynamics to keep the ion inertia and finite-gyroradius effects while a guiding-center–drift approximation is used for the motion of electrons.[3] Conducting walls are assumed for the electrostatic field and the particles are elastically reflected back at the wall. The simulation parameters are the following: aspect ratio $R_0/a=3$, safety factor $q=1.1(1+2.5r^2/a^2)$ which corresponds to a current profile of $j_\varphi\sim(1+2.5r^2/a^2)^{-2}$. Initially, electrons and ions have a local Maxwellian velocity distribution with the density profile taken to be $n_e(r)=n_i(r)=n_0\exp(-4r^2/a^2)$. The initial electron-temperature profile is chosen similarly to provide $\eta_e\equiv d(\ln T_e)/d(\ln n_e)=1$ everywhere. The initial ion temperature is taken to be uniform. The average density and temperature are specified by choosing $\Omega_e/\langle\omega_{pe}\rangle=5$, $m_i/m_e=100$, $\langle T_e\rangle/T_i=4$, and $\langle\lambda_e\rangle/\Delta=2$, where $\Omega_e$ is evaluated at the magnetic axis, $\Delta$ is the grid size, and $\langle\,\rangle$ means average over the entire plasma volume. These parameters correspond to low-density tokamak discharges in laboratory experiments. In the cross section, a $64\times64$ ($L^2$) spatial grid is used for numerical computation with its physical length $L/\rho_i=32$, $\rho_i=(2T_i/m_i)^{1/2}/\Omega_i$. Seven Fourier modes, $n=0,\pm1,\pm2,\pm3$, are kept in the toroidal direction. The electron-ion pitch-angle scattering is simulated by Monte Carlo collision model[5] where the collision frequency $\nu_{ei}$ for an electron goes as $v^{-3}$ and $v$ is the speed of the electron. The collision frequency is chosen such that $\nu_e^*\equiv\nu_{\rm eff}/\omega_{be}$ ($\nu_{\rm eff}=\nu_{ei}/\epsilon$ is the effective-collision frequency and $\omega_{be}=\sqrt{\epsilon}V_e/qR_0$ is the electron-bounce frequency) decreases from $\nu_e^*\approx10$ at $r/a\approx0.8$ to 0.2 at $r/a\approx0.25$ and then increases toward the center of the plasma column, suggesting that the bulk of the plasma is in the banana and the plateau regimes corresponding to high-temperature tokamak experiments.

Figure 1(a) shows the time development of the electric field energy for different $m$ modes with $n=2$ ($m,n$ are the poloidal- and toroidal-mode numbers), radial mode structure in Fig. 1(b), and poloidal mode structure in Fig. 1(c). The

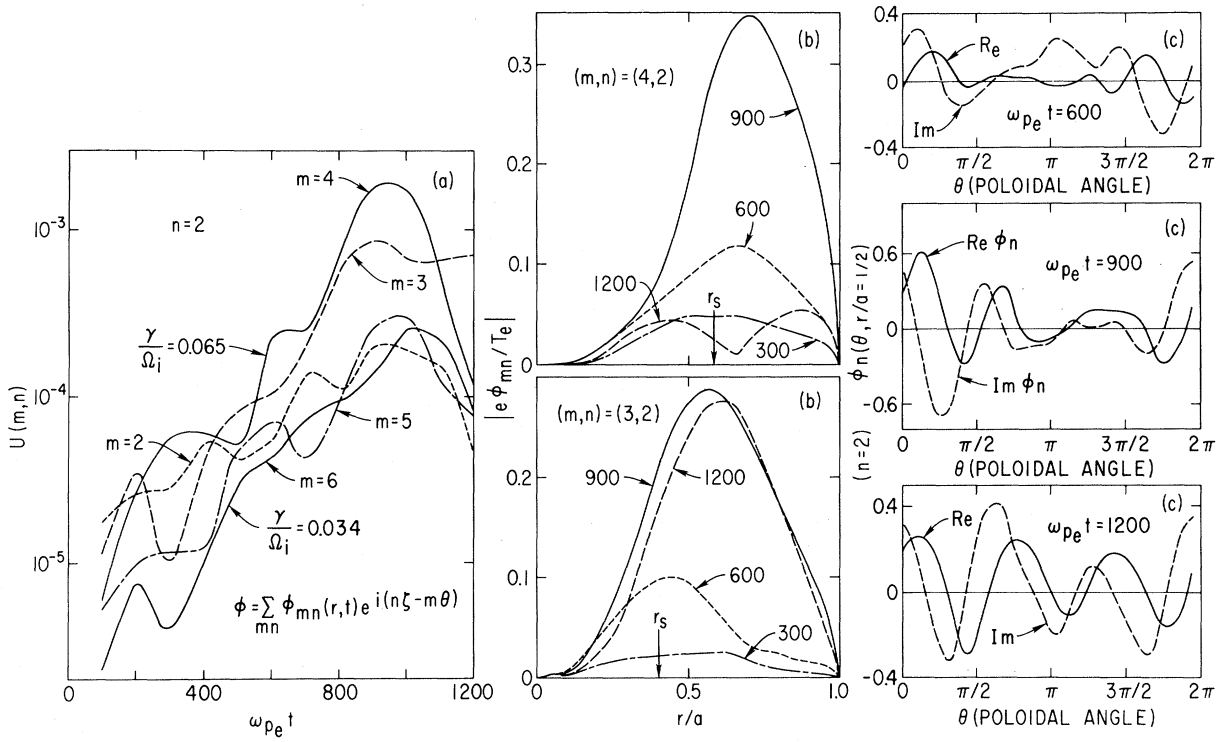


FIG. 1. (a) Temporal evolution of the trapped-electron instability for several modes with $n=2$. (b) Radial mode structure for the (4,2) and (3,2) modes at different times. (c) Poloidal mode structure at $r/a=0.5$ and $n=2$ at different times.

growth rates of the unstable modes are about $\gamma/\Omega_i = 0.03-0.07$ for the modes shown and these growth rates are within a factor of 1.5 from the prediction of the two-dimensional linear theory.[2] Since the aspect ratio is small ($R/a=3$), toroidal coupling is strong for various $m$ modes causing them to grow at about the same growth rate. These unstable modes grow about two orders of magnitude and saturate. The dominant mechanism for saturation is due to density and electron-temperature diffusion which results from the generation of convective cells ($\omega \simeq 0$), strong plasma turbulence, and hence the broad spectrum ($\Delta\omega \approx \omega$).

Radial mode structures for $(m,n)=(4,2)$ and (3,2) shown in Fig. 1(b) are localized around the rational surface at $r/a \approx 0.5$ during the linear stage. Near saturation, the maximum amplitude reaches $e\varphi_{mn}/T_e \approx 0.3$ and the mode extends nearly over the entire plasma column. The peak of the amplitude shifts slightly outwards in the nonlinear stage.

Poloidal mode structure shown in Fig. 1(c) at $r/a=0.5$ and $n=2$ indicates clearly the ballooning effect in the linear stage where the mode amplitude is larger at the outside ($\theta=0$) than the inside ($\theta=\pi$) of a torus. When the instability enters into a nonlinear stage ($\omega_{pe}t \gtrsim 1000$), however, Fig. 1(c) indicates that the ballooning effect almost disappeared and the amplitude is nearly constant along the field lines. The reason for this is that the plasma is already in a strong turbulent state in which stable modes as well as convective cells are excited by nonlinear mode-coupling processes as seen for the drift turbulence.[6] Under such conditions, ballooning effects become less prominent since the mode-coupling process makes the spectrum isotropic and the nonlinearly generated broad spectrum (convective cells) does not require the presence of trapped particles.

Figure 2 indicates the frequency and wave-number spectra for the turbulence generated. Time evolution of the electric field energy with respect to poloidal-mode number $|E(m)|^2$ averaged over the plasma radius and toroidal angle is shown in Fig. 2(a). We observe that the spectral distribution is more or less monotonic with $m$, consistent with recent measurements in the PLT (Princeton Large Torus) tokamak.[1] The relatively large amplitude for $m=1$ at early times is due to the $\nabla B$ drifts of the ions which can generate $(m,n)=(1,0)$. At the time of saturation,

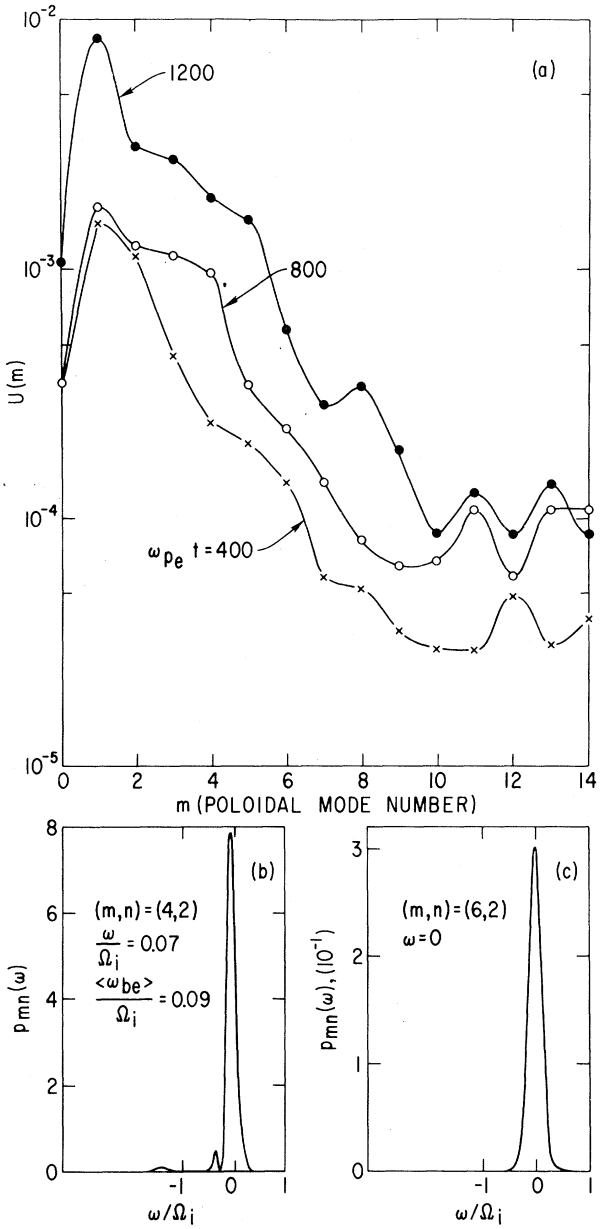


FIG. 2. (a) Temporal evolution of the spectral distribution with $k_\perp$. (b), (c) Frequency spectrum for the (4, 2) and (6, 2) modes at $r/a = 0.47$.

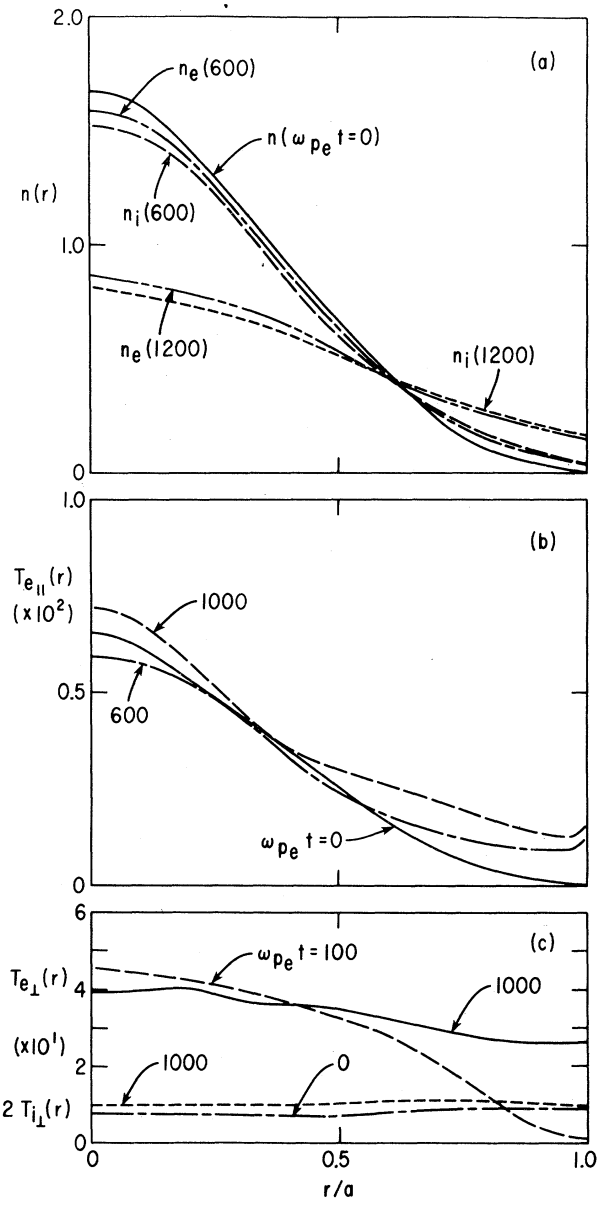


FIG. 3. (a) Particle diffusion for the ions and electrons. Electron- and ion-temperature diffusion (b) parallel and (c) perpendicular to the magnetic field.

not only the most unstable trapped-particle modes with $m = 3-8$, but also the $m = 1, 2$ modes, grow to large amplitudes. This is the sign of a broad spectrum of the frequency consistent with the generation of strong plasma turbulence and convective cells.

Frequency spectra of the (4, 2) and (6, 2) modes are shown in Figs. 2(b) and 2(c). For the (4, 2) mode the measurement was performed near its rational surface at $r/a = 0.47$. Observed frequency $\omega/\Omega_i = 0.07$ is close to the prediction from linear theory[2] and the spectrum is broad ($\Delta\omega \approx \omega$). For the (6, 2) mode, the observation point is far away from its rational surface and, in fact, the observed frequency is peaked at zero although the amplitude is considerably smaller. This is one of the examples of strong plasma turbulence which can generate convective cells.

Figure 3 shows the gross particle diffusion (a) and electron heat transport (b) and (c) associ-

ated with the instabilities. Relatively small particle and temperature diffusion, observed in the linear stage of the instability, is enhanced rapidly near saturation which leads to the stabilization of the system. The observed particle diffusion is about $D_\perp \approx 2\times 10^{-2}\rho_i^2\omega_{pe}$ close to the theoretical estimate $D_\perp \approx (cT_e/eB)(\rho_i/L_n)$ based on the strong plasma turbulence and convective cells for drift wave turbulence.[4]

Electron temperature diffusion perpendicular and parallel to the confining magnetic field is shown in Fig. 3 where the diffusion of $T_{\perp e}$ is larger than the density diffusion by a factor of 3–4. The parallel temperature diffusion is, on the other hand, much smaller. This is because the high-energy electrons trapped in a magnetic mirror $[v_\perp > \epsilon^{-1/2} v_\parallel]$ preferentially diffuse out because of plasma turbulence, resulting in large $T_{\perp e}$ diffusion. Heating of the parallel temperature at the outer side of the torus $(r/a \gtrsim 0.5)$ is partly due to the anomalous diffusion and partly due to electron pitch-angle scattering which makes the electron velocity distribution isotropic. The total running time of the simulation is, however, only one or two collision times for the electron-temperature relaxation, and the complete isotropization has not yet been reached.

We have also studied the TEM modes by varying the initial electron-temperature profile so that $\eta_e = 0, -1$. Simulation results show that for $\eta_e = 0$ the instabilities become less unstable with a growth rate about a factor of 3 smaller than the case for $\eta_e = 1$. For $\eta_e = -1$, we found that the system becomes completely stable and no instabilities were observed, consistent with the prediction of linear theory.

In conclusion, dissipative trapped-electron instabilities have been studied successfully using a three-dimensional toroidal particle simulation model. Anomalous diffusion of heat and particles are observed, which is consistent with a previous estimate.[4] In addition, the observed generation of strong plasma turbulence is consistent with the measurements from laboratory experiments[1] and mode-coupling calculations.[6] Ballooning structure, which is the characteristic feature of the trapped-particle mode, is found to diminish at the strongly turbulent nonlinear stage.

While the present simulation work is for the initial-value problem, it revealed several important physical processes such as observation of a broad spectrum, strong plasma turbulence, and anomalous transport associated with the trapped-electron instabilities. These processes are inherent in laboratory plasma where a steady state is established through balance of energy input and anomalous transport.

We acknowledge many useful discussions with Dr. G. Rewoldt and Dr. P. H. Rutherford. This work was supported by U. S. Department of Energy Contract No. EY-76-C-02-3073.

[1]E. Mazzucato, Phys. Rev. Lett. 36, 792 (1976); C. M. Surko and R. E. Slusher, Phys. Rev. Lett. 37, 1747, (1976), and 38, 258(E) (1976); M. Okabayashi and V. Arunasalam, Nucl. Fusion 17, 497 (1977).

[2]B. B. Kadomtsev and O. P. Pogutse, Nucl. Fusion 11, 67 (1971); G. Rewoldt, W. M. Tang, and E. A. Frieman, in Proceedings of the Annual Controlled Fusion Theory Meeting, Gatlinburg, Tennessee, 26–28 April 1978 (to be published), Paper E9.

[3]C. Z. Cheng and H. Okuda, J. Comp. Phys. 25, 133 (1977).

[4]C. Z. Cheng and H. Okuda, Phys. Rev. Lett. 38, 708 1037(E) (1977), and Nucl. Fusion 18, 587 (1978).

[5]R. Shanny, J. M. Dawson, and J. M. Greene, Phys. Fluids 10, 1281 (1967).

[6]C. Z. Cheng and H. Okuda, in Proceedings of the Annual Controlled Fusion Theory Meeting, Gatlinburg, Tennessee, 26–28 April 1978 (to be published), Paper OB4.